Electronic Supplementary Material (ESI) for Chemical Communications
This journal is © The Royal Society of Chemistry 2011

Supporting Information

Nonheme Ferric Hydroperoxo Intermediates Are Efficient Oxidants of Bromide Oxidation

Anil Kumar Vardhaman,[a] Chivukula V. Sastri,*[a] Devesh Kumar,*[b] and Sam P. de Visser*[c]

[a] Department of Chemistry, Indian Institute of Technology Guwahati, Assam 781039, India.
[b] Department of Applied Physics, School for Physical Sciences, Babasaheb Bhimrao Ambedkar University, Vidya Vihar, Rai Bareilly Road, Lucknow 226 025, India.
[c] Manchester Interdisciplinary Biocentre and the School of Chemical Engineering and Analytical Science The University of Manchester 131 Princess Street, Manchester M1 7DN, United Kingdom

This journal is © The Royal Society of Chemistry 2011

Methods.

Experimental Conditions:

Materials: All chemicals obtained from Aldrich Chemical Co. were the best available purity and were used without further purification unless otherwise indicated. Solvents were dried according to published procedures[1] and distilled under argon prior to use. Iodosylbenzene was prepared by a literature method.[2] Iron(II) complexes such as $[Fe^{II}(N4Py)](CF_3SO_3)_2$,[3] and $[Fe^{II}(Bn\text{-}tpen)](CF_3SO_3)_2$,[4] were prepared in a glove-box following a procedure reported in the literature. Iron(IV)-oxo complexes, including $[Fe^{IV}{=}O(N4Py)]^{2+}$ and $[Fe^{IV}{=}O(Bn\text{-}tpen)]^{2+}$,[5] were prepared by reacting their corresponding iron(II) complexes with PhIO in CH_3CN at ambient temperature. The low spin ferric hydroperoxo complexes were generated in situ using H_2O_2 (10 equiv) in CH_3OH as reported earlier.[6]

Instrumentation: UV-vis spectra were recorded on a Hewlett Packard 8453 spectrophotometer equipped with either constant temperature circulating water bath or a liquid nitrogen cryostat (Unisoku) with a temperature controller. Electrospray ionization mass spectra (ESI-MS) were recorded on a Waters (Micromass MS Technologies) Q-TOF Premier mass spectrometer by infusing samples directly into the source at 15 μL/min using a syringe pump. The spray voltage was set at 2 kV and the capillary temperature at 80 °C.

Reactivity Studies: All reactions were run in a 10 mm path length UV cuvette by monitoring UV-vis spectral changes of reaction solutions. The rate constants were determined by fitting the changes in absorbance of the intermediates under study. Reactions were run at least in triplicate, and the data reported represent the average of these reactions.

DFT calculations:

All calculations use procedures we previously employed for calculations on $[Fe(IV){=}O(N4Py)]^{2+}$ and $[Fe(IV){=}O(Bn\text{-}tpen)]^{2+}$ and their reactivity patterns.[7] Geometries were fully optimized using density functional theory methods as implemented in *Gaussian*-09,[8] and utilize the unrestricted hybrid density functional B3LYP.[9] We used a Los Alamos type double-ζ quality basis set on Fe that contains a core potential,[10] an aug-cc-pV5Z-PP basis set on bromine,[11] and 6-31G on the rest of the atoms: basis set B1.[12] Subsequent single point calculations used the LACV3P+ basis set with core potential on Fe, an aug-cc-pV5Z-PP basis set on Br, and 6-311+G* on the rest of the atoms: basis set B2. Our calculated models were $[Fe^{III}OOH(N4Py)\text{---}Br^-]^+$ and $[Fe^{III}OOH(Bn\text{-}tpen)\text{---}Br^-]^+$, and due to the charge distributions in these models we decided to do full geometry optimizations and frequencies using the continuum polarized conductor model (CPCM)[13] as implemented in *Gaussian*-09 using either acetonitrile or methanol as the solvent. All geometries were fully optimized without geometric constraints. The local minima are characterized with real frequencies only, whereas the transition states had one imaginary frequency for the correct mode. Transition states were located by first running detailed geometry scans between reactants and products with the reaction coordinate fixed at specific intervals, while optimization the rest of the geometry. The maximum of these scans was then used as a starting point for a full transition state geometry optimization.

This journal is © The Royal Society of Chemistry 2011

References:

1. *Purification of Laboratory Chemicals*; W. L. F. Armarego, D. D. Perrin (Eds.); Pergamon Press: Oxford, 1997.
2. *Organic Syntheses*, H. Saltzman, J. G. Sharefkin (Eds.); Wiley, New York, 1973, Collect. Vol. V, pp. 658.
3. M. Lubben, A. Meetsma, E. C. Wilkinson, B. Feringa, L. Que, Jr., *Angew. Chem. Int. Ed. Engl*., 1995, **34**, 1512.
4. L. Duelund, R. Hazell, C. J. McKenzie, L. P. Nielsen, H. Toftlund, *J. Chem. Soc., Dalton Trans*., 2001, 152.
5. J. Kaizer, E. J. Klinker, N. Y. Oh, J.-U. Rohde, W. J. Song, A. Stubna, J. Kim, E. Münck, W. Nam, L. Que, Jr., *J. Am. Chem. Soc*., 2004, **126**, 472.
6. A. Hazell, C. J. McKenzie, L. P. Nielsen, S. Schindler, M. Weitzer, *J. Chem. Soc., Dalton Trans*., 2002, 310–317.
7. (a) D. Kumar, H. Hirao, L. Que Jr., S. Shaik, *J. Am. Chem. Soc*., 2005, **127**, 8026–8027. (b) H. Hirao, D. Kumar, L. Que Jr., S. Shaik, *J. Am. Chem. Soc*., 2006, **128**, 8590–8606.
8. *Gaussian*-09, Revision B.01, M. J. Frisch, G. W. Trucks, H. B. Schlegel, G. E. Scuseria, M. A. Robb, J. R. Cheeseman, G. Scalmani, V. Barone, B. Mennucci, G. A. Petersson, H. Nakatsuji, M. Caricato, X. Li, H. P. Hratchian, A. F. Izmaylov, J. Bloino, G. Zheng, J. L. Sonnenberg, M. Hada, M. Ehara, K. Toyota, R. Fukuda, J. Hasegawa, M. Ishida, T. Nakajima, Y. Honda, O. Kitao, H. Nakai, T. Vreven, J. A. Montgomery, Jr., J. E. Peralta, F. Ogliaro, M. Bearpark, J. J. Heyd, E. Brothers, K. N. Kudin, V. N. Staroverov, T. Keith, R. Kobayashi, J. Normand, K. Raghavachari, A. Rendell, J. C. Burant, S. S. Iyengar, J. Tomasi, M. Cossi, N. Rega, J. M. Millam, M. Klene, J. E. Knox, J. B. Cross, V. Bakken, C. Adamo, J. Jaramillo, R. Gomperts, R. E. Stratmann, O. Yazyev, A. J. Austin, R. Cammi, C. Pomelli, J. W. Ochterski, R. L. Martin, K. Morokuma, V. G. Zakrzewski, G. A. Voth, P. Salvador, J. J. Dannenberg, S. Dapprich, A. D. Daniels, O. Farkas, J. B. Foresman, J. V. Ortiz, J. Cioslowski, and D. J. Fox, Gaussian, Inc., Wallingford CT, 2010.
9. A. D. Becke, *J. Chem. Phys*., 1993, **98**, 5648–5652. (b) C. Lee, W. Yang, R. G. Parr, *Phys. Rev. B*, 1988, **37**, 785–789.
10. P. J. Hay, W. R. Wadt, *J. Chem. Phys*., 1985, **82**, 270–283.
11. K. A. Peterson, B. C. Shepler, D. Figgen, H. Stoll, *J. Phys. Chem. A*, 2006, **110**, 13877.
12. W. J. Hehre, R. Ditchfield, J. A. Pople, *J. Chem. Phys.*, 1972, **56**, 2257–2261.
13. (a) M. Cossi, N. Rega, G. Scalmani, and V. Barone, *J. Comp. Chem*., 2003, **24**, 669–681. (b) V. Barone and M. Cossi, *J. Phys. Chem. A*, 1998, **102**, 1995–2001.

Table S1. Absolute energies (in au) and relative energies (in kcal mol^{-1}) of [Fe^{III}OOH(Bn-tpen)---Br^{-}]$^{+}$ (^{2,4,6}R$_{2a}$) reactant complexes as obtained in *Gaussian*-09.

UB3LYP/B1 results						
Multip	E	E+ZPE	G	ΔE[a]	ΔE+ZPC[a]	ΔG[a]
M2	-2011.072385	-2010.526217	-2010.591214	0.00	0.00	0.00
M4	-2011.050888	-2010.507463	-2010.574400	13.49	11.77	10.55
M6	-2011.054107	-2010.511993	-2010.581113	11.47	8.93	6.34

[a] Relative energies with respect to ^{2}R$_{2a}$.

	UB3LYP/B2//UB3LYP/B1 results			
Multip	E	E+ZPE	ΔE[a]	ΔE+ZPC[a]
M2	-2011.788820	-2011.242652	0.00	0.00
M4	-2011.760180	-2011.216754	17.97	16.25
M6	-2011.769882	-2011.227768	11.88	9.34

[a] Relative energies with respect to ^{2}R$_{2a}$.

Table S2. Group spin densities and group charges of UB3LYP/B1 optimized geometries.

	Spin densities					Charges				
	Fe	O1	OH	Br	Bntpen	Fe	O1	OH	Br	Bntpen
M2	0.89	0.18	0.02	0.00	-0.08	0.77	-0.36	0.05	-1.01	1.55
M4	2.93	-0.02	-0.04	0.00	0.13	0.88	-0.36	0.06	-1.01	1.43
M6	3.95	0.45	0.11	0.00	0.49	0.97	-0.39	0.11	-0.98	1.29

Table S3. Group spin densities and group charges of UB3LYP/B2//UB3LYP/B1 results.

	Spin densities					Charges				
	Fe	O1	OH	Br	Bntpen	Fe	O1	OH	Br	Bntpen
M2	0.92	0.17	0.02	0.00	-0.11	-1.28	0.55	0.10	-0.96	2.58
M4	3.06	-0.01	-0.04	0.00	-0.01	-0.87	0.39	0.07	-0.95	2.36
M6	4.04	0.39	0.10	0.00	0.46	-0.99	0.73	0.21	-0.91	1.97

This journal is © The Royal Society of Chemistry 2011

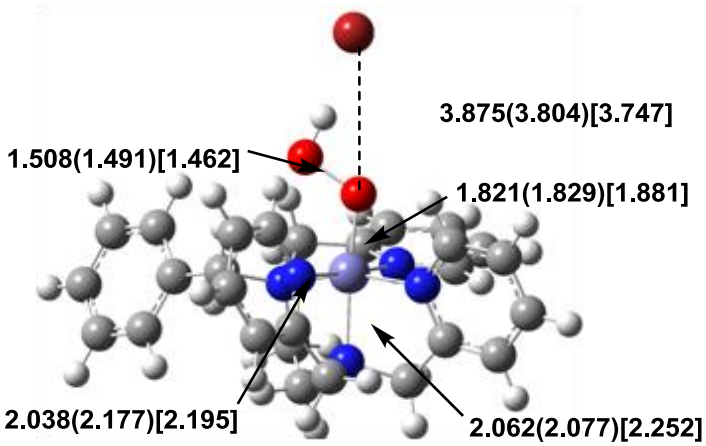

Figure S1. Optimized UB3LYP/B1 geometry of $^{2}R_{2a}$ ($^{4}R_{2a}$) [$^{6}R_{2a}$] with bond lengths in angstroms.

This journal is © The Royal Society of Chemistry 2011

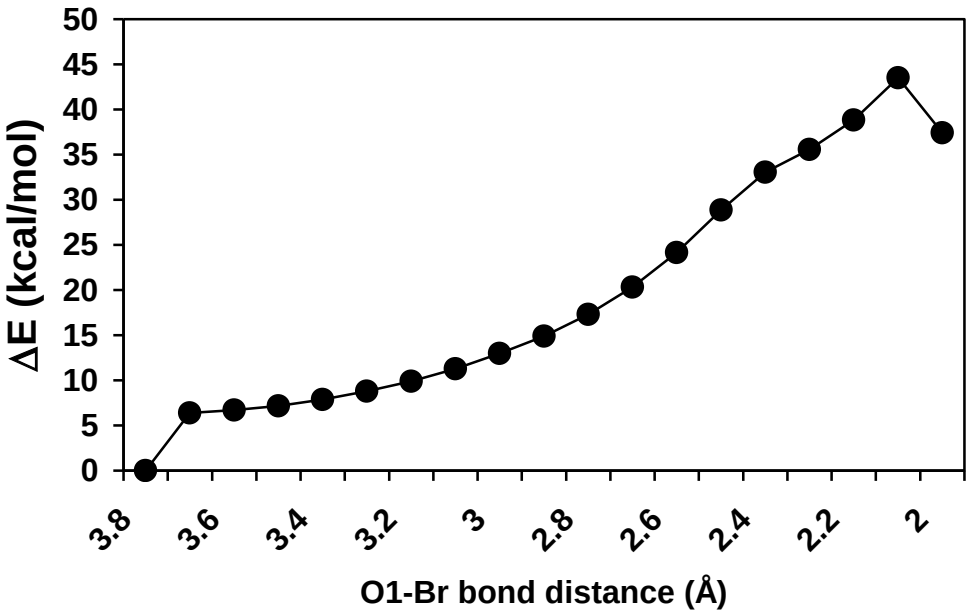

Figure S2. Geometry scan for the oxygen atom transfer reaction to Br^- by $^2R_{2a}$. Energies are in kcal mol^{-1} relative to $^2R_{2a}$.

Table S4. Absolute energies (in au) and relative energies (in kcal mol^{-1}) of oxygen atom transition state (^{2,4,6}TS$_{Br,2a}$) obtained in *Gaussian*-09.

UB3LYP/B1 result						
Multip	E	E+ZPE	G	ΔE[a]	ΔE+ZPC[a]	ΔG[a]
M2	-2010.999334	-2010.457052	-2010.519245	45.84	43.40	45.16
M4	-2010.991084	-2010.450786	-2010.516926	51.02	47.33	46.62
M6	-2011.015365	-2010.476066	-2010.545406	35.78	31.47	28.74

[a] Relative energies with respect to ^{2}R$_{2a}$.

UB3LYP/B2//UB3LYP/B1 result.				
Multip	E	E+ZPE	ΔE[a]	ΔE+ZPC[a]
M2	-2011.713522	-2011.171240	47.25	44.81
M4	-2011.690059	-2011.149760	61.97	58.29
M6	-2011.717805	-2011.178505	44.56	40.25

[a] Relative energies with respect to ^{2}R$_{2a}$.

Table S5. Group spin densities and group charges of UB3LYP/B1 optimized geometries.

	Spin densities					Charges				
	Fe	O1	OH	Br	Bntpen	Fe	O1	OH	Br	Bntpen
M2	0.06	0.29	0.12	0.52	0.01	0.50	-0.38	-0.01	-0.25	1.13
M4	2.03	0.32	0.35	0.29	0.01	0.57	-0.33	-0.08	-0.24	1.08
M6	3.77	0.46	0.20	0.37	0.21	0.75	-0.26	-0.09	-0.39	0.99

Table S6. Group spin densities and group charges of UB3LYP/B2//UB3LYP/B1 results.

	Spin densities					Charges				
	Fe	O1	OH	Br	Bntpen	Fe	O1	OH	Br	Bntpen
M2	0.11	0.15	0.13	0.59	0.01	-0.95	0.46	-0.15	-0.31	1.94
M4	2.13	0.22	0.36	0.37	-0.08	-0.50	0.10	-0.41	-0.16	1.96
M6	3.88	0.36	0.24	0.47	0.04	-0.54	0.01	-0.26	-0.37	2.17

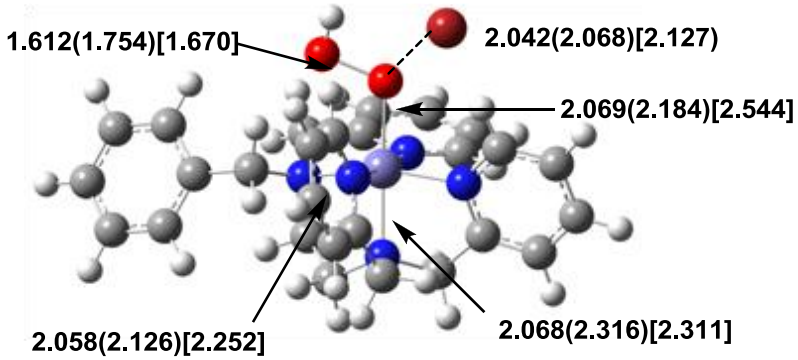

*i*305.7 (*i*576.7) [*i*444.6] cm^{-1}

Figure S3. Optimized UB3LYP/B1 geometry of $^{2}TS_{Br,2a}$ ($^{4}TS_{Br,2a}$) [$^{6}TS_{Br,2a}$] with bond lengths in angstroms.

Table S7. Absolute energies (in au) and relative energies (in kcal mol^{-1}) of [Fe^{III}OH(Bn-tpen)---OBr^{-}]$^{+}$ (^{2,4,6}P$_{2a}$) intermediate complex as obtained in Gaussian-09.

UB3LYP/B1 result						
Multip	E	E+ZPE	G	ΔE[a]	ΔE+ZPC[a]	ΔG[a]
M2	-2011.017544	-2010.475859	-2010.539203	34.41	31.60	32.64
M4	-2011.008088	-2010.468523	-2010.534255	40.35	36.20	35.74
M6	-2011.021043	-2010.482511	-2010.551379	32.22	27.43	25.00

[a] Relative energies with respect to ^{2}R$_{2a}$.

	UB3LYP/B2//UB3LYP/B1			
Multip	E	E+ZPE	ΔE[a]	ΔE+ZPC[a]
M2	-2011.726454	-2011.184768	39.14	36.32
M4	-2011.706607	-2011.167042	51.59	47.45
M6	-2011.723411	-2011.184879	41.04	36.25

[a] Relative energies with respect to ^{2}R$_{2a}$.

Table S8. Group spin densities and group charges of UB3LYP/B1 optimized geometries.

	Spin densities					Charges				
	Fe	O1	OH	Br	Bntpen	Fe	O1	OH	Br	Bntpen
M2	0.06	0.27	0.69	-0.01	-0.01	0.43	-0.32	-0.13	-0.10	1.13
M4	1.96	0.31	0.75	-0.01	-0.01	0.52	-0.34	-0.08	-0.15	1.05
M6	3.79	0.33	0.69	0.00	0.20	0.61	-0.34	-0.13	-0.13	0.99

Table S9. Group spin densities and group charges of UB3LYP/B2//UB3LYP/B1 results.

	Spin densities					Charges				
	Fe	O1	OH	Br	Bntpen	Fe	O1	OH	Br	Bntpen
M2	0.09	0.28	0.62	0.01	0.00	-0.95	0.00	-0.26	0.00	2.20
M4	2.07	0.29	0.71	0.02	-0.08	-0.70	-0.24	-0.24	0.00	2.19
M6	3.99	0.27	0.61	0.06	0.07	-0.82	-0.02	-0.29	-0.04	2.17

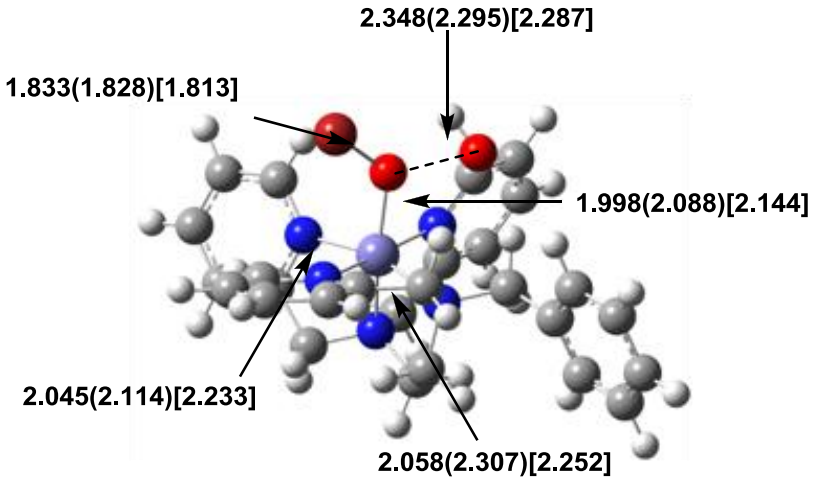

Figure S4. Optimized UB3LYP/B1 geometry of $^{2}P_{2a}$ ($^{4}P_{2a}$) [$^{6}P_{2a}$] with bond lengths in angstroms.

Table S10. Absolute energies (in au) and relative energies (in kcal mol^{-1}) of [Fe^{III}OOH(N4Py)---Br^{-}]$^{+}$ (^{2,4,6}R$_{1a}$) reactant complex as obtained in Gaussian-09.

UB3LYP/B1 result						
Multip	E	E+ZPE	G	ΔE[a]	ΔE+ZPC[a]	ΔG[a]
M2	-1853.871946	-1853.443022	-1853.502292	0.00	0.00	0.00
M4	-1853.828345	-1853.400410	-1853.460789	27.36	26.74	26.04
M6	-1853.853550	-1853.428399	-1853.491596	11.54	9.18	6.71

[a] Relative energies with respect to ^{2}R$_{1a}$.

	UB3LYP/B2//UB3LYP/B1 result			
Multip	E	E+ZPE	ΔE[a]	ΔE+ZPC[a]
M2	-1854.521632	-1854.092708	0.00	0.00
M4	-1854.464217	-1854.036283	36.03	35.41
M6	-1854.501601	-1854.076451	12.57	10.20

[a] Relative energies with respect to ^{2}R$_{1a}$.

Table S11. Group spin densities and group charges of UB3LYP/B1 optimized geometries.

	Spin densities					Charges				
	Fe	O1	OH	Br	N4py	Fe	O1	OH	Br	N4py
M2	0.80	0.23	0.03	0.00	-0.06	0.77	-0.36	0.05	-1.00	1.54
M4	2.64	0.33	0.03	0.00	0.00	0.85	-0.41	0.03	-1.02	1.54
M6	3.96	0.44	0.11	0.00	0.50	1.03	-0.41	0.11	-0.97	1.24

Table S12. Group spin densities and group charges of UB3LYP/B2//UB3LYP/B1 results.

	Spin densities					Charges				
	Fe	O1	OH	Br	N4py	Fe	O1	OH	Br	N4py
M2	0.82	0.24	0.02	0.00	-0.08	-2.24	0.26	0.25	-0.95	3.69
M4	2.78	0.31	0.02	0.00	-0.11	-2.19	0.03	0.21	-0.97	3.92
M6	4.04	0.41	0.09	0.00	0.46	-3.70	0.39	0.27	-0.92	4.97

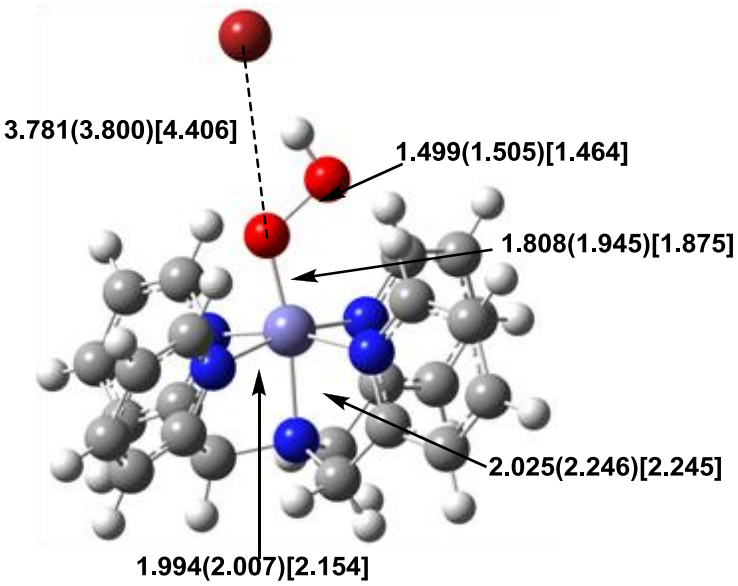

Figure S5. Optimized UB3LYP/B1 geometry of $^{2}R_{1a}$ ($^{4}R_{1a}$) [$^{6}R_{1a}$] with bond lengths in angstroms.

This journal is © The Royal Society of Chemistry 2011

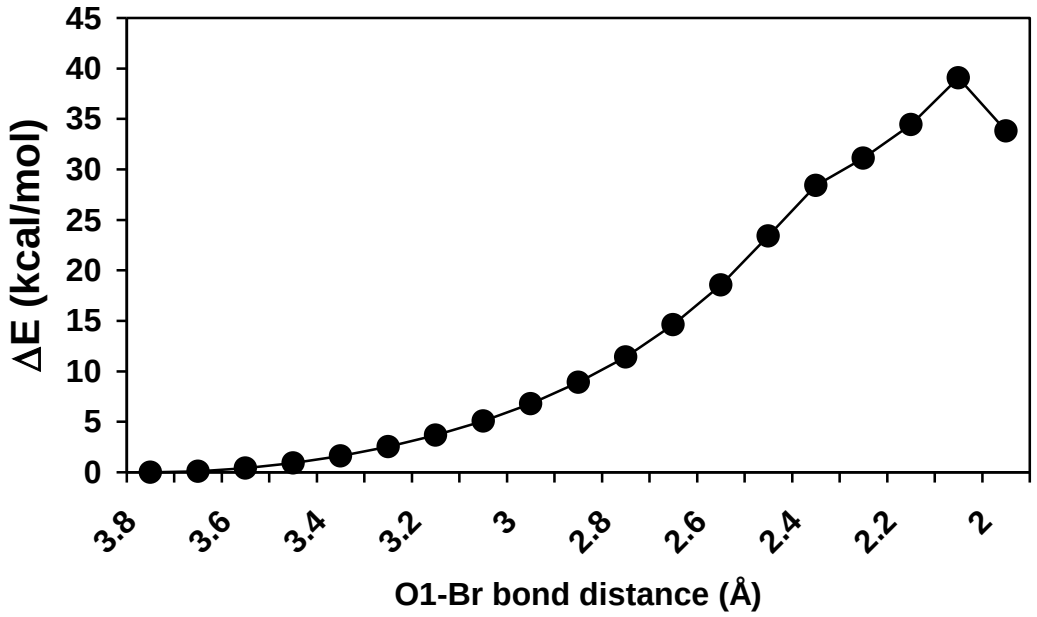

Figure S6. Geometry scan for the oxygen atom transfer reaction to Br^- by $^2R_{1a}$. Energies are in kcal mol^{-1} relative to $^2R_{1a}$.

Table S13. Absolute energies (in au) and relative energies (in kcal mol^{-1}) of oxygen atom transfer transition state ($^{2,4,6}TS_{Br,1a}$) as obtained in Gaussian-09.

UB3LYP/B1 result						
Multip	E	E+ZPE	G	ΔE^a	$\Delta E+ZPC^a$	ΔG^a
M2	-1853.806326	-1853.380771	-1853.437165	41.18	39.06	40.87
M4	-1853.790438	-1853.365705	-1853.426034	51.15	48.52	47.85
M6	-1853.821014	-1853.397550	-1853.457529	31.96	28.53	28.09

[a] Relative energies with respect to $^2R_{1a}$.

UB3LYP/B2//UB3LYP/B1 result				
Multip	E	E+ZPE	ΔE^a	$\Delta E+ZPC^a$
M2	-1854.454081	-1854.028526	42.39	40.28
M4	-1854.427582	-1854.002849	59.02	56.39
M6	-1854.463259	-1854.039795	36.63	33.20

[a] Relative energies with respect to $^2R_{1a}$.

Table S14. Group spin densities and group charges of UB3LYP/B1 optimized geometries.

	Spin densities					Charges				
	Fe	O1	OH	Br	N4py	Fe	O1	OH	Br	N4py
M2	0.06	0.29	0.11	0.53	0.00	0.52	-0.40	0.00	-0.27	1.15
M4	1.98	0.44	-0.01	0.59	0.00	0.60	-0.38	0.01	-0.32	1.09
M6	3.85	0.47	0.02	0.37	0.29	0.82	-0.36	0.07	-0.59	1.06

Table S15. Group spin densities and group charges of UB3LYP/B2//UB3LYP/B1 results.

	Spin densities					Charges				
	Fe	O1	OH	Br	N4py	Fe	O1	OH	Br	N4py
M2	0.11	0.14	0.12	0.61	0.02	-1.43	0.07	-0.01	-0.37	2.75
M4	2.07	0.34	0.01	0.67	-0.08	-1.57	0.02	0.04	-0.55	3.06
M6	4.00	0.34	0.05	0.42	0.19	-1.66	0.32	0.02	-0.87	3.18

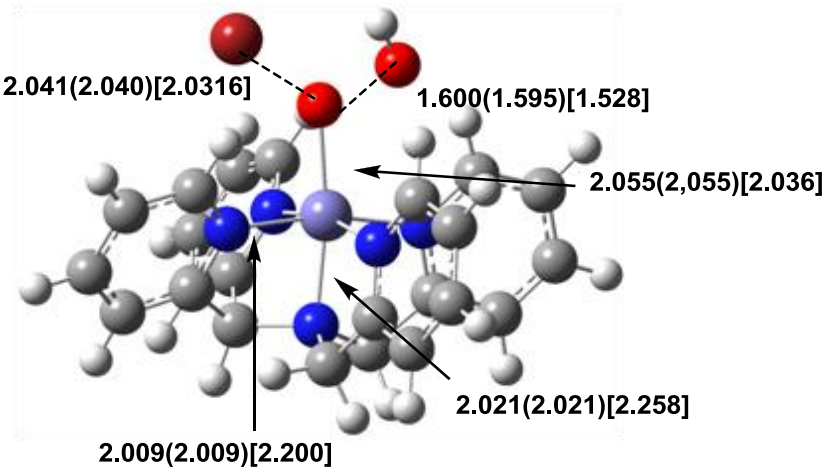

*i*210.2 (*i*191.7) [*i*113.6] cm^{-1}

Figure S7. Optimized UB3LYP/B1 geometry of $^{2}TS_{Br,1a}$ ($^{4}TS_{Br,1a}$) [$^{6}TS_{Br,1a}$] with bond lengths in angstroms.

Table S16. Absolute energies (in au) and relative energies (in kcal mol^{-1}) of [Fe^{III}OH(N4Py)---OBr^{-}]$^{+}$ (^{2,4,6}P$_{1a}$) intermediate complex as obtained in Gaussian-09.

UB3LYP/B1 results						
Multip	E	E+ZPE	G	ΔE[a]	ΔE+ZPC[a]	ΔG[a]
M2	-1853.822821	-1853.398267	-1853.456234	30.83	28.08	28.90
M4	-1853.802811	-1853.380536	-1853.442518	43.38	39.21	37.51
M6	-1853.822285	-1853.401013	-1853.464596	31.16	26.36	23.65

[a] Relative energies with respect to ^{2}R$_{1a}$.

UB3LYP/B2//UB3LYP/B1 results				
Multip	E	E+ZPE	ΔE[a]	ΔE+ZPC[a]
M2	-1854.465100	-1854.040546	35.47	32.73
M4	-1854.432420	-1854.010145	55.98	51.81
M6	-1854.458539	-1854.037267	39.59	34.79

[a] Relative energies with respect to ^{2}R$_{1a}$.

Table S17. Group spin densities and group charges of UB3LYP/B1 optimized geometries.

	Spin densities					Charges				
	Fe	O1	OH	Br	N4py	Fe	O1	OH	Br	N4py
M2	0.05	0.26	0.71	-0.01	-0.01	0.52	-0.33	-0.11	-0.21	1.12
M4	1.97	0.27	0.78	0.00	-0.02	0.61	-0.36	-0.06	-0.24	1.05
M6	3.74	0.29	0.79	0.02	0.17	0.68	-0.42	-0.06	-0.12	0.91

Table S18. Group spin densities and group charges of UB3LYP/B2//UB3LYP/B1 results.

	Spin densities					Charges				
	Fe	O1	OH	Br	N4py	Fe	O1	OH	Br	N4py
M2	0.08	0.25	0.66	0.02	-0.01	-1.19	-0.57	-0.23	-0.01	3.00
M4	2.08	0.25	0.75	0.05	-0.12	-1.14	-0.46	-0.15	-0. 0.0402	2. 2.5176
M6	3.87	0.25	0.75	0.07	0.06	-0.81	-0.56	-0.17		

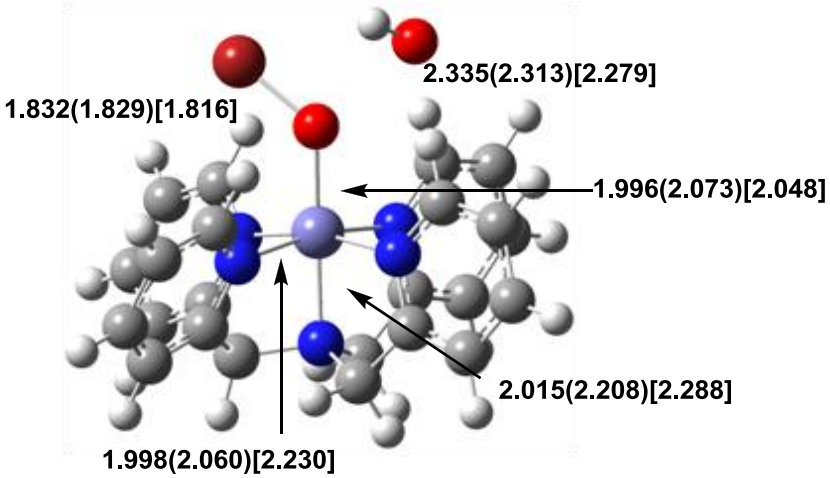

Figure S8. Optimized UB3LYP/B1 geometry of $^{2}P_{1a}$ ($^{4}P_{1a}$) [$^{6}P_{1a}$] with bond lengths in angstroms.

Table S19. Absolute energies (in au) and relative energies (in kcal mol^{-1}) of [Fe^{III}OOH(Bn-tpen)---Br^{-}]$^{+}$ (^{2,4,6}R$_{2a}$) reactant complex as obtained in *Gaussian*-09.

	UB3LYP/B2//UB3LYP/B1 in Methanol results			
Multip	E	E+ZPE	ΔE[a]	ΔE+ZPC[a]
M2	-2011.765399	-2011.219231	0.00	0.00
M4	-2011.759818	-2011.216392	3.50	1.78
M6	-2011.769500	-2011.227386	-2.57	-5.12

[a] Relative energies with respect to ^{2}R$_{2a}$.

Table S20. Group spin densities and group charges of UB3LYP/B2//UB3LYP/B1 in Methanol results.

	Spin densities					Charges				
	Fe	O1	OH	Br	Bntpen	Fe	O1	OH	Br	Bntpen
M2	0.93	0.17	0.02	0.00	-0.12	-1.30	0.51	0.10	-0.96	2.64
M4	3.06	-0.01	-0.04	0.00	-0.01	-0.87	0.39	0.07	-0.95	2.36
M6	4.04	0.39	0.10	0.00	0.46	-0.99	0.73	0.21	-0.91	1.97

Table S21. Absolute energies (in au) and relative energies (in kcal mol^{-1}) of oxygen atom transition state (^{2,4,6}TS$_{Br,2a}$) obtained in *Gaussian*-09.

	UB3LYP/B2//UB3LYP/B1 in Methanol results			
Multip	E	E+ZPE	ΔE[a]	ΔE+ZPC[a]
M2	-2011.697307	-2011.155025	42.73	40.29
M4	-2011.689861	-2011.149562	47.40	43.72
M6	-2011.717579	-2011.178279	30.01	25.70

[a] Relative energies with respect to ^{2}R$_{2a}$.

Table S22. Group spin densities and group charges of UB3LYP/B2//UB3LYP/B1 in Methanol results.

	Spin densities					Charges				
	Fe	O1	OH	Br	Bntpen	Fe	O1	OH	Br	Bntpen
M2	0.11	0.15	0.13	0.59	0.01	-0.97	0.44	-0.16	-0.28	1.98
M4	2.13	0.22	0.36	0.37	-0.08	-0.50	0.10	-0.41	-0.16	1.96
M6	3.88	0.36	0.24	0.47	0.04	-0.54	0.01	-0.27	-0.37	2.16

Table S23. Absolute energies (in au) and relative energies (in kcal mol^{-1}) of [Fe^{III}OH(Bn-tpen)---OBr^{-}]$^{+}$ (^{2,4,6}P$_{2a}$) intermediate complex as obtained in Gaussian-09.

	UB3LYP/B2//UB3LYP/B1 in Methanol results			
Multip	E	E+ZPE	ΔE[a]	ΔE+ZPC[a]
M2	-2011.714015	-2011.172329	32.24	29.43
M4	-2011.706421	-2011.166856	37.01	32.87
M6	-2011.723204	-2011.184672	26.48	21.69

[a] Relative energies with respect to ^{2}R$_{2a}$.

Table S24. Group spin densities and group charges of UB3LYP/B2//UB3LYP/B1 in Methanol results.

	Spin densities					Charges				
	Fe	O1	OH	Br	Bntpen	Fe	O1	OH	Br	Bntpen
M2	0.09	0.28	0.61	0.01	0.00	-1.00	0.00	-0.26	0.01	2.25
M4	2.07	0.29	0.71	0.02	-0.08	-0.70	-0.24	-0.24	0.00	2.19
M6	3.99	0.27	0.61	0.06	0.07	-0.82	-0.02	-0.29	-0.04	2.17

Table S25. Absolute energies (in au) and relative energies (in kcal mol^{-1}) of [Fe^{III}OOH(N4Py)---Br^{-}]$^{+}$ (^{2,4,6}R$_{1a}$) reactant complex as obtained in Gaussian-09.

	UB3LYP/B2//UB3LYP/B1 in Methanol results			
Multip	E	E+ZPE	ΔE[a]	ΔE+ZPC[a]
M2	-1854.506063	-1853.959895	0.00	0.00
M4	-1854.463777	-1853.920351	26.54	24.81
M6	-1854.501208	-1853.959094	3.05	0.50

[a] Relative energies with respect to ^{2}R$_{1a}$.

Table S26. Group spin densities and group charges of UB3LYP/B2//UB3LYP/B1 in Methanol results.

	Spin densities					Charges				
	Fe	O1	OH	Br	Bntpen	Fe	O1	OH	Br	Bntpen
M2	0.84	0.23	0.02	0.00	-0.09	-2.30	0.22	0.25	-0.95	3.77
M4	2.78	0.31	0.02	0.00	-0.11	-2.19	0.03	0.21	-0.97	3.92
M6	4.04	0.41	0.09	0.00	0.46	-3.70	0.39	0.27	-0.92	4.97

Table S27. Absolute energies (in au) and relative energies (in kcal mol^{-1}) of oxygen atom transfer transition state (^{2,4,6}TS$_{Br,1a}$) as obtained in Gaussian-09.

	UB3LYP/B2//UB3LYP/B1 in Methanol results			
Multip	E	E+ZPE	ΔE[a]	ΔE+ZPC[a]
M2	-1854.435803	-1853.893521	44.09	41.65
M4	-1854.427333	-1853.887034	49.40	45.72
M6	-1854.463002	-1853.923702	27.02	22.71

[a] Relative energies with respect to ^{2}R$_{1a}$.

Table S28. Group spin densities and group charges of UB3LYP/B2//UB3LYP/B1 in Methanol results.

	Spin densities					Charges				
	Fe	O1	OH	Br	Bntpen	Fe	O1	OH	Br	Bntpen
M2	0.11	0.13	0.13	0.61	0.02	-1.46	0.05	-0.03	-0.35	2.78
M4	2.07	0.34	0.01	0.67	-0.08	-1.57	0.02	0.04	-0.55	3.06
M6	4.00	0.34	0.46	0.00	0.19	-1.65	0.32	0.02	-0.87	3.18

Table S29. Absolute energies (in au) and relative energies (in kcal mol^{-1}) of [Fe^{III}OH(N4Py)---OBr^{-}]$^{+}$ (^{2,4,6}P$_{1a}$) intermediate complex as obtained in Gaussian-09.

	UB3LYP/B2//UB3LYP/B1 in Methanol results			
Multip	E	E+ZPE	ΔE[a]	ΔE+ZPC[a]
M2	-1854.450639	-1853.908953	34.78	31.97
M4	-1854.432217	-1853.892652	46.34	42.20
M6	-1854.458348	-1853.919816	29.94	25.15

[a] Relative energies with respect to ^{2}R$_{1a}$.

Table S30. Group spin densities and group charges of UB3LYP/B2//UB3LYP/B1 in Methanol results.

	Spin densities					Charges				
	Fe	O1	OH	Br	Bntpen	Fe	O1	OH	Br	Bntpen
M2	0.08	0.26	0.65	0.02	-0.01	-1.23	-0.57	-0.24	0.00	3.05
M4	2.08	0.25	0.75	0.05	-0.12	-1.14	-0.46	-0.14	-0.02	2.76
M6	3.87	0.25	0.75	0.07	0.06	-0.81	-0.56	-0.17	0.04	2.51

This journal is © The Royal Society of Chemistry 2011

FeOOH -> FeO + OH scan for ^{2}N4py-FeOOH

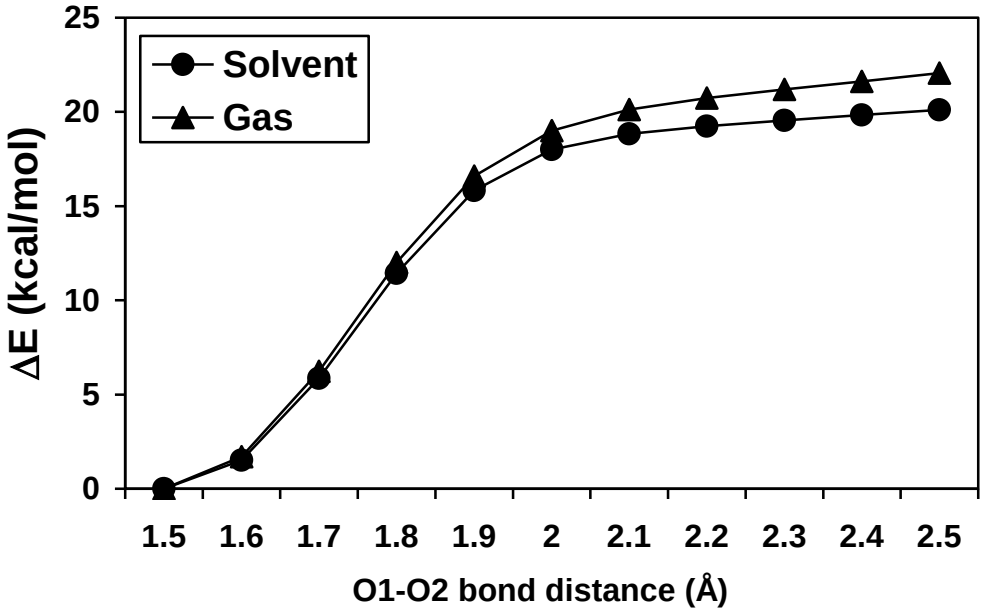

FeOOH -> FeO + OH scan for ^{4,6}N4py-FeOOH

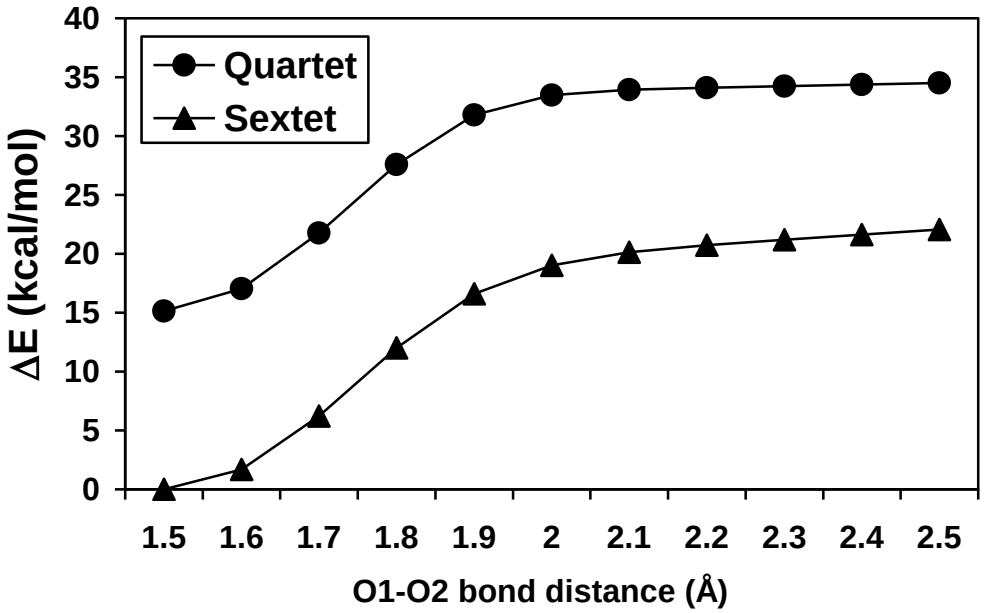

This journal is © The Royal Society of Chemistry 2011

FeOOH -> FeO + OH scan for ^{2}Bntpen-FeOOH

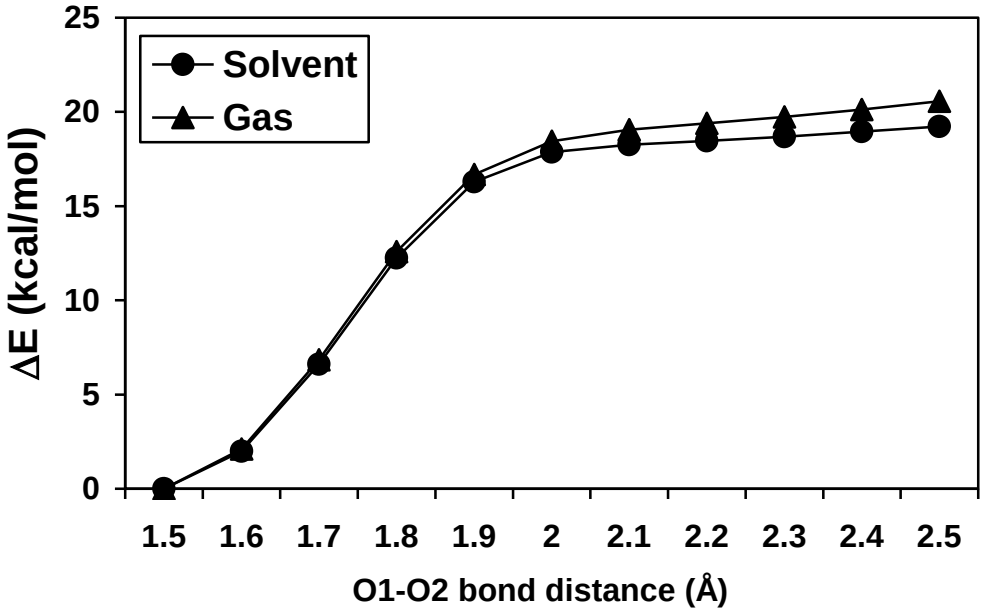

FeOOH -> FeO + OH scan for ^{4,6}Bntpen-FeOOH

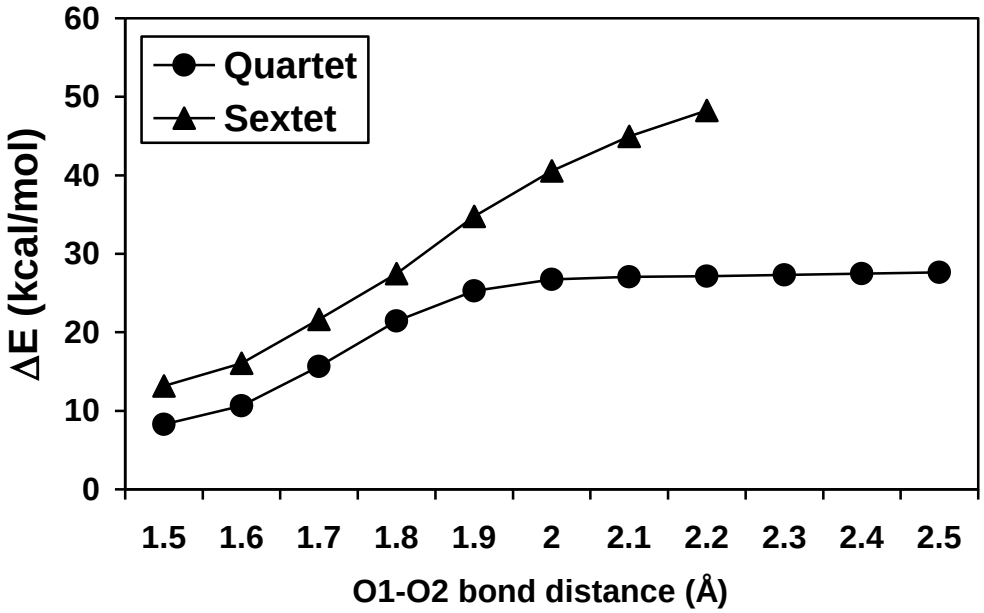

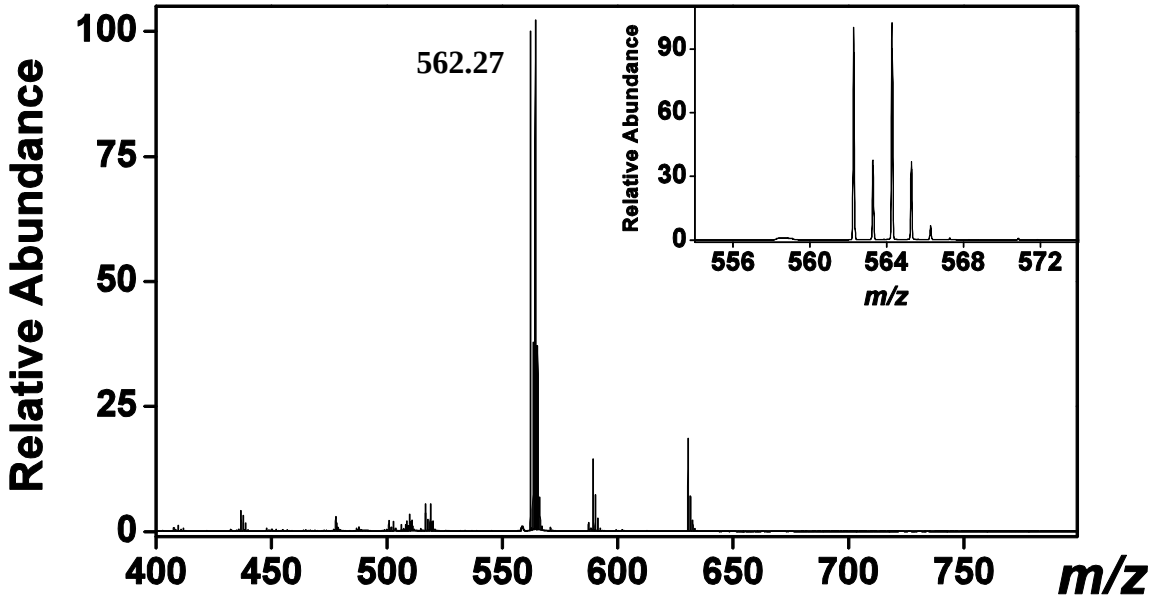

Figure S9 ESI-MS taken after the completion of the reaction of **1b** with TBABr in CH_3CN at RT. A mass peak at *m/z* of 562.27 is assigned to $[Fe^{III}(OH)(N4Py)Br]^+$, Insets shows the isotopic distribution in the region of *m/z* 560–568.

This journal is © The Royal Society of Chemistry 2011

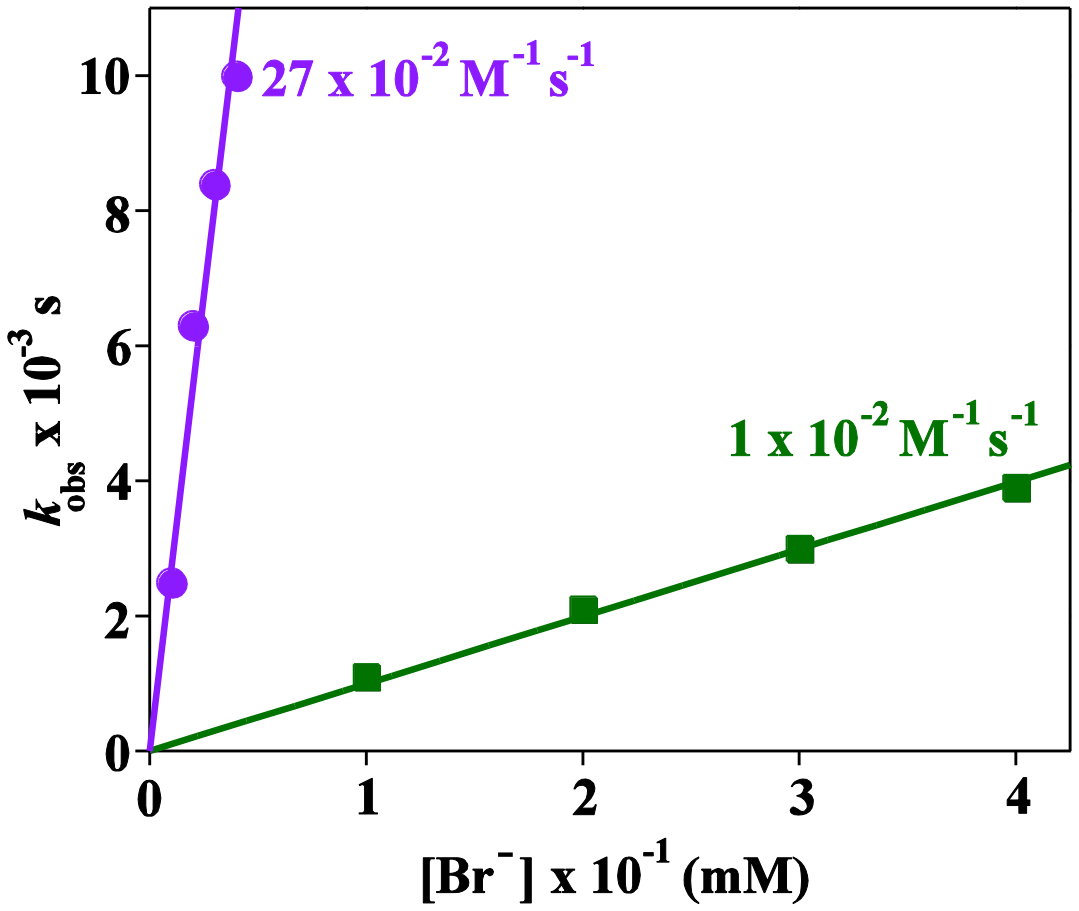

Figure S10. Comparison of second order rate constants as determined in the reactions of **2b**, 1×10^{-2} M^{-1} s^{-1} (●, green) and **2a**, 27×10^{-2} M^{-1} s^{-1} (■, purple) with TBABr at –20 ^{0}C.

This journal is © The Royal Society of Chemistry 2011

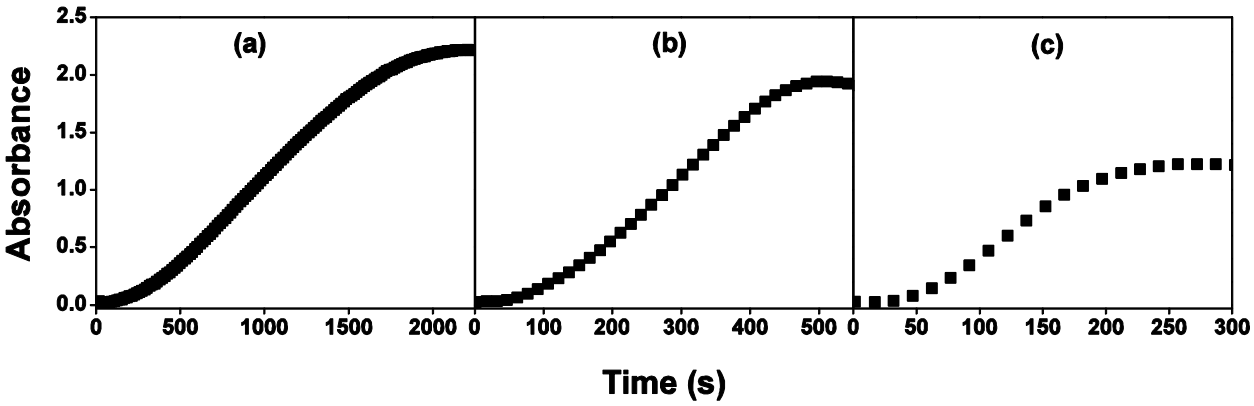

Figure S11. Time course for the reaction of bromophenol blue in the presence of (a) 0.05 mM, (b) 0.10 mM and (c) 0.15 mM of $[Fe^{II}(N4Py)]^{2+}$, TBABr (80 mM), phenol red (62.5 μM).